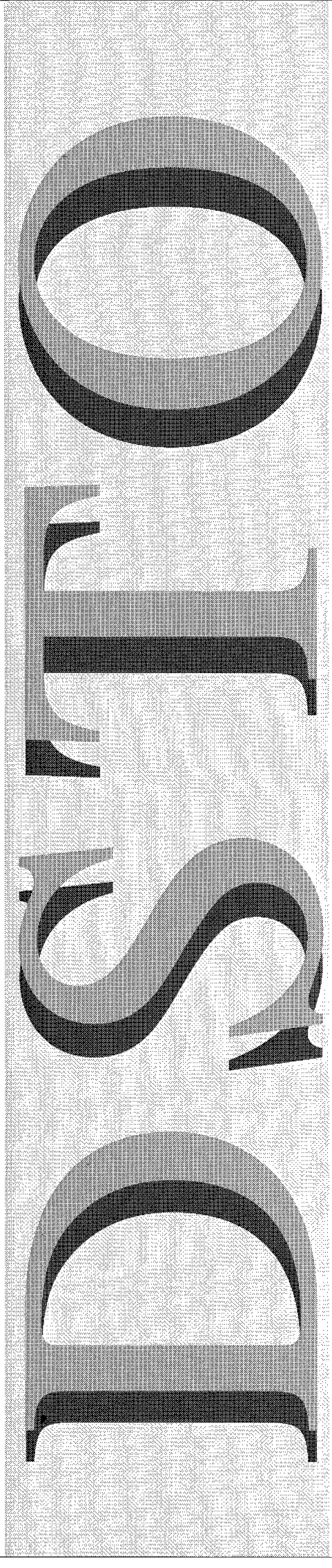

An Approach to Characterising Ground Probing Radar Target Echoes for Landmine Recognition

Dragana Carevic

DSTO-TR-0680

DEPARTMENT OF DEFENCE

DEFENCE SCIENCE AND TECHNOLOGY ORGANISATION

AN APPROACH TO CHARACTERISING GROUND PROBING RADAR TARGET ECHOES FOR LANDMINE RECOGNITION

Dragana Carevic

Tactical Surveillance Systems Division
Electronics and Surveillance Research Laboratory

DSTO–TR–0680

ABSTRACT

This report investigates an approach to characterising Ground Probing Radar (GPR) backscatter echoes from landmines using linear combinations of exponentially damped sinusoids. The GPR signatures of surrogate landmines and PVC cylinders buried in dry sand are measured using an impulse radar system with centre frequency of 1.4 GHz and a 90% bandwidth. The GPR signal parameters are represented as sets of complex poles computed from a series of neighbouring signatures recorded over each target type. The algorithm proposed by Kumaresan and Tufts which uses backward linear prediction and the low-rank data matrix approximation based on singular value decomposition is applied to this computation.

The performance of the Kumaresan and Tufts (KT) algorithm is compared with that of the Prony method when both techniques are applied to modelling simulated signals. It is concluded that the KT method provides more stable pole estimates.

Two approaches to determining the order of the model are examined and compared for simulated and real data.

The results show that the poles corresponding to different target types form clusters in the two-dimensional α-f space (where α is the pole damping factor and f is the pole frequency). This indicates that these pole clusters can be used for the recognition of landmines.

APPROVED FOR PUBLIC RELEASE

DEPARTMENT OF DEFENCE

DEFENCE SCIENCE AND TECHNOLOGY ORGANISATION

Published by

DSTO Electronics and Surveillance Research Laboratory
PO Box 1500
Salisbury, South Australia, Australia 5108

Telephone: *(08) 8259 5555*
Facsimile: *(08) 8259 6567*

AR No. AR-010-~~555~~ 561
June, 1998

APPROVED FOR PUBLIC RELEASE

An Approach to Characterising Ground Probing Radar Target Echoes for Landmine Recognition

EXECUTIVE SUMMARY

Modern anti-personnel landmines have a minimal metallic content which makes detection using electromagnetic induction (EMI) detectors very difficult, if not impossible. To detect even a low-metallic-content mine the detector threshold must be set so low that many false alarms occur. DSTO is investigating the use of Ground Probing Radar (GPR) as a means of detecting non-metallic landmines and identifying mines with a metal content. The GPR used is a centimetre resolution short range radar. Target responses consist of a set of reflections from dielectric surfaces in the ground and in targets as well as the metal components within targets.

This report investigates an approach to characterising GPR backscatter signals from landmines as linear combinations of exponentially damped sinusoids. The targets used in the experiments are surrogate landmines and PVC cylinders of various sizes. The targets are buried in dry sand and the measurements were made using a 1.4 GHz centre frequency antenna with 90% bandwidth.

Two methods for computing the signal parameters (poles) are compared using the simulated data contaminated by white Gaussian noise: the Prony method and a method proposed by Kumaresan and Tufts (KT). The KT algorithm, which applies backward linear prediction and the low-rank data matrix approximation based on singular value decomposition, is found to give more stable pole estimates. This method is, therefore, applied to model the real target signatures where the signal poles are computed using a series of neighbouring GPR signatures recorded over each target type. Both raw and background-removed GPR target signatures were used.

Two different approaches for the model order selection are also investigated: 1) an information-theoretic approach and 2) an approach based on the thresholding of singular values of the data matrix. While the information-theoretic criterion was successful for the simulated data, the simpler thresholding approach has been found to give better results for modelling real signals. The poles computed using the KT algorithm and this latter approach were stable for a range of threshold values.

The results of this initial study show that the poles corresponding to different target types form clusters in the two-dimensional α-f space (where α is the pole damping factor and f is the pole frequency). It is therefore expected that such poles can be used for the recognition of landmines. However, further research is needed to confirm these results.

THIS PAGE IS INTENTIONALLY BLANK

Authors

Dragana Carevic
Tactical Surveillance Systems Division

Dragana Carevic received BSc. and M.S. degrees in Electrical Engineering from Belgrade University in 1983 and 1989, respectively. From 1983 to 1991 she worked as a Research Engineer in the Electrical Engineering Institute "Nikola Tesla" in Belgrade on the development of intelligent instrumentation for signal measurement, processing and recognition. In 1996 she received a PhD degree from Curtin University in the areas of image processing and analysis. Her research interests include signal and image processing, pattern recognition and data fusion.

THIS PAGE IS INTENTIONALLY BLANK

Contents

Figures

Tables

1 Introduction

Detection and identification of buried landmines is an important yet difficult task. Standard countermine methods that use electromagnetic induction (EMI) can easily locate metallic objects. However, most contemporary landmines are characterised by a low metallic content and EMI detectors often fail to locate such devices. Recent developments in Ground Probing Radar (GPR) which utilise short duration pulses (0.1-1 ns) offer a promising new approach to this problem. In this situation antenna and target are located in half-spaces having different electromagnetic properties. The backscattered echoes which are usually distorted by multiple scattering are used for target identification (see Daniels *et al.* [1] and Daniels [2] for a comprehensive review of current GPR techniques and their applications). A serious drawback of the GPR system is that it is limited in ability to discriminate between landmine and non-landmine echoes. Advanced signal processing and target classification techniques are sought with the aim of solving this problem. It is also expected that improved detection/recognition performance can be achieved through combining different types of sensors, such as EMI detector, GPR, and infrared imagery.

This report is exclusively concerned with the information that can be extracted from the GPR backscattered target echoes. The approach is to model separate backscattered GPR echoes from a landmine target as a linear combination of exponential functions $\exp(st)$. The complex parameters (*i.e.*, poles) s are expected to be characteristic for each target-type, and invariant with respect to target orientation. This approach was first applied to the problem of free space scattering from resonant bodies [3]. Chan *et al.* [4, 5] have demonstrated that similar technique can be successfully applied to identifying buried plastic (dielectric) mine-like targets. Other approaches include extinction-pulse (E-pulse) or kill-pulse (K-pulse) methods [6, 7, 8] applied to free-space scattering, and methods utilising artificial neural networks [9, 10] and time-frequency analysis [11] as applied to the GPR backscattered target echoes.

Previous work was mainly concerned with large targets so that the pulse lengths were a fraction of the target size. By contrast the targets investigated in this report are small anti-personnel mines of sizes similar to the pulse length in air.

The outline of this report is as follows. Section 2 describes the methods applied for modelling of the GPR signals. In particular, Section 2.1 presents the KT algorithm for estimating the parameters of the exponentially damped sinusoid model. Section 2.2 describes the two methods for selecting the model order used by the KT algorithm. Section 3 provides information on the GPR system measurements and the investigated targets and Section 4 presents the results of experiments in signal modelling using simulated and real data. Concluding remarks and recommendations for the future research work on landmine recognition based on the GPR echoes are presented in Section 5.

2 Theoretical Background

The problem of parameter estimation of exponentially damped sinusoids is very important in many applications. A simple and widely used technique is the Prony method [12].

However, as it is based on linear least-squares, the standard Prony method is highly sensitive to the additive measurement noise. It also requires knowing the number of damped exponentials contained in the sum (*i.e.*, the order of the model) M in advance. Several procedures to refine the Prony method have been proposed [13, 14]. In particular, the approach described in [13] based on the principal-component analysis, has been applied to modelling the GPR backscattered echoes (see [15]). Unfortunately, the author has found that the poles estimated using this technique are highly unstable.

The method proposed by Kumaresan and Tufts [16] offers an improved performance when applied to signals with lower signal-to-noise ratio (SNR) and compares favorably with Prony. It uses backward linear prediction and low-rank data matrix approximation based on singular value decomposition (SVD). In this report the KT algorithm is applied to modelling the GPR echoes from our targets.

Other techniques for estimating the parameters of the assumed model from the measured data include "pencil-of-function" methods [17, 18], maximum likelihood approaches [19], techniques based on the total least squares [20, 21] and higher-order correlations [22]. Barone *at al.* [23] proposed an approach for modelling time-varying signals by which the observed interval is divided into several short segments, each of which is then modelled separately.

2.1 Kumaresan and Tufts Algorithm

Consider a data sequence $x(n)$ which consists of M exponentially damped sinusoidal signals:

$$x(n) = \sum_{k=1}^{M} C_k \exp(s_k n) \tag{1}$$

where C_k's are non-zero complex amplitudes and $s_k = -\alpha_k + j\omega_k$ are complex poles for $k = 1, \ldots, M$. α_k's are the pole damping factors ($\alpha_k > 0$), and $\omega_k = 2\pi f_k$, where f_k's are the pole frequencies. Let $y(n)$ be an observed sequence corrupted by additive white Gaussian noise $v(n)$

$$y(n) = x(n) + v(n) \quad \text{for} \quad n = 0, 1, 2, \ldots, N-1, \quad N > 2M.$$

For the data sequence $y(n)$ backward linear prediction equations in matrix form are given as:

$$\begin{vmatrix} y^*(1) & y^*(2) & \ldots & y^*(L) \\ y^*(2) & y^*(3) & \ldots & y^*(L+1) \\ \vdots & \vdots & \ddots & \vdots \\ y^*(N-L) & y^*(N-L+1) & \ldots & y^*(N-1) \end{vmatrix} \begin{vmatrix} c(1) \\ c(2) \\ \vdots \\ c(L) \end{vmatrix} = - \begin{vmatrix} y^*(0) \\ y*(1) \\ \vdots \\ y^*(N-L-1) \end{vmatrix} \tag{2}$$

or, equivalently,

$$\mathbf{A_b c} = -\mathbf{h} \tag{3}$$

where $\mathbf{A_b}$ is the $(N-L)$x(L) backward data matrix, $\mathbf{c}$ is backward linear prediction filter and "$*$" denotes complex conjugation. The above equation can be written in an augmented form as,

$$\mathbf{A'_b c'} = \mathbf{0} \tag{4}$$

with $\mathbf{A}'_\mathbf{b} = (\mathbf{h}|\mathbf{A_b})$ and $\mathbf{c}' = (\mathbf{1}, \mathbf{c^T})^\mathbf{T}$, where $\mathbf{c}'$ is the prediction-error filter and "T" denotes matrix transpose. If the data is noiseless, the prediction-error filter polynomial

$$B(z) = 1 + c(1)z^{-1} + c(2)z^{-2} + \ldots + c(L)z^{-L} \tag{5}$$

has zeros at $e^{-s_k^*}$ for $k = 1, 2, \ldots, M$, provided that the order of the backward linear prediction equations in Eq.(2) L is chosen such that $M \leq L \leq N - M$ [24]. These M zeros are the signal zeros and fall outside the unit circle as the consequence of the fact that data is used in the reverse direction to compute $\mathbf{c}'$ in Eq.(2). If $L > M$, polynomial $B(z)$ (5) has additional $L - M$ zeros, which are called extraneous zeros. In this case Eq.(2) has more than one solution since the rank of $\mathbf{A_b}$ (or $\mathbf{A}'_\mathbf{b}$) is $M(< L)$. It has been shown [24] that there exists a unique, minimum-norm, solution to Eq.(2) for which all $L - M$ extraneous zeros fall within the unit circle provided that data is noiseless. This solution corresponds to the least squares solution.

In this way it is possible to identify the M signal zeros, lying outside the unit circle, as opposed to the $L - M$ extraneous zeros. Moderately large values of L have been found essential in improving the accuracy of the pole location estimates [16]. (Note that, for $L = M$ and forward instead of backward prediction in Eq.(2), this technique is equivalent to the standard Prony method).

In the presence of additive noise the least squares solution to Eq.(2) is ill-conditioned and introduces considerable perturbations in the solution vector $\mathbf{c}$[1]. To alleviate this problem Kumaresan and Tufts [16] used the truncated SVD to increase the SNR in the data prior to obtaining the solution vector $\mathbf{c}$. Namely, SVD of the data matrix $\mathbf{A_b}$ is given as:

$$\mathbf{A_b} = U \begin{bmatrix} \mathbf{\Sigma} \\ \mathbf{0} \end{bmatrix} V^T \tag{6}$$

where U is an $(N - L)$x$(N - L)$ dimensional matrix of left singular vectors, V is an LxL dimensional matrix of right singular vectors and Σ is a diagonal matrix of singular values $\{\sigma_i\}_{i=1}^{L}$. If the measurements are noiseless, *i.e.*, if $y(n) = x(n)$, where $x(n)$ is defined by Eq.(1), then matrix $\mathbf{A_b}$ has rank M and only M singular values of $\mathbf{A_b}$ are nonzero. In the presence of noise and model mismatch however the matrix $\mathbf{A_b}$ will have full rank, but will be "close" to a matrix $\mathbf{A}^\circ_\mathbf{b}$ of the rank M, and thus $\sigma_{M+1} \approx \sigma_{M+2} \approx \cdots \approx \sigma_L \approx 0$. Consequently, Kumaresan and Tufts used the optimum rank M approximation of $\mathbf{A}$ obtained by setting $L - M$ smaller singular values of $\mathbf{A}$ to zero, and computed the solution vector $\mathbf{c}$ as,

$$\mathbf{c} = -\sum_{\mathbf{k=1}}^{\mathbf{M}} \sigma_\mathbf{k}^{-1} \mathbf{v_k u_k^T h} \tag{7}$$

where $\{\sigma_1, \sigma_2, \ldots, \sigma_M\}$ are M largest singular values of $\mathbf{A}$, $\{u_1, u_2, \ldots, u_M\}$ are corresponding left singular vectors, and $\{v_1, v_2, \ldots, v_M\}$ are the right singular vectors.

Once signal poles are computed, complex amplitudes C_k can be found using linear least-squares approach which involves minimising the following squared-error sum:

$$E = \sum_{n=1}^{N} |y(n) - \sum_{k=1}^{M} C_k \exp(s_k n)|^2 \tag{8}$$

[1]Least squares solution to Eq.(2) can be obtained by matrix inversion using singular value decomposition.

2.2 Choosing the Order of the Model

Equation Eq.(7) requires that the order of the model (or, simply, the model) M is known. However, in practice the correct model M is not known *a priori* and has to be estimated. This estimate can be obtained using singular values of the data matrix $\mathbf{A_b}$. Following the discussion about the properties of the singular values of the matrix $\mathbf{A_b}$ corresponding to a noisy signal (see Section 2.1), a simple way to adaptively determine the order of the model involves choosing M such that σ_{M+1} is the first singular value smaller than $t\sigma_1$, where the constant t is chosen from the interval $(0, 1)$ and the singular values are ordered in decreasing order.

Several more complex criteria based on the application of information-theoretic principles to model selection are also available (see [25] page 548 for more details). The popular methods are the Akaike information criterion (AIC) [26] and the minimum description length criterion (MDL) [27] defined, respectively, as:

$$AIC = -2\ln(f(\mathbf{y}|\hat{\theta})) + 2d \quad (9)$$

$$MDL = -2\ln(f(\mathbf{y}|\hat{\theta})) + d\ln N. \quad (10)$$

Here $f(\mathbf{y}|\hat{\theta})$ is the maximum likelihood function of the observation vector $\mathbf{y}$, θ is the parameter set of the model in Eq.(1) and d is the number of free parameters in θ. N in Eq.(10) denotes the total number of observations in $\mathbf{y}$. Both AIC and MDL select the model which minimises the corresponding equation above.

In this report we apply an approach for determining AIC and MDL which is matched to the methods based on SVD and thus can be used along with the KT algorithm involving very little extra computation [28].

3 GPR Measurements and Targets

In the experiments we used an FR-127-MSCB MK2 impulse GPR system developed by CSIRO [29]. The system collects 127 echoes, or soundings, per second and each sounding is composed of 512 samples of 12 bit accuracy. The sounding range is variable between 4 ns and 32 ns. The system uses bistatic bow-tie antennas with the transmit pulse created by a fast-recovery diode at the transmit antenna. Centre frequency and bandwidth of the transmitted pulse can be changed by changing the antenna. In this report we utilise the soundings obtained using the antenna with 1.4 GHz centre frequency and the bandwidth of 1.136 GHz.

Six targets were measured (see Table 1). Three of these targets were surrogate landmines developed by the DSTO countermine research project [30]. These targets, denoted as ST-AP(1), ST-AP(2) and ST-AP(3), are the surrogate anti-personnel mines modelled after the M14, PMN and PMN2 blast mines, respectively. The PMN and PMN2 are anti-personnel mines with non-metallic casings which have been encountered by the Australian troops attached to the United Nations de-mining operations in Cambodia and Afghanistan. The M14 is a very small anti-personnel mine with almost no metal content and very small size. As such it is a very difficult target for GPR landmine detection. Three simple test targets, PVC (poly-vinyl chloride) cylinders, were also measured.

LIST OF TARGETS

Target Designation	Target Description	Target Orientation
PVC Test Target 1	Solid PVC Cylinder, 5.2 cm in diameter and 10.1 cm high	Not critical, target symmetric
PVC Test Target 2	Solid PVC Cylinder, 10.35 cm in diameter and 5.05 cm high	Not critical, target symmetric
PVC Test Target 3	Solid PVC Cylinder, 15.35 cm in diameter and 5.05 cm high	Not critical, target symmetric
ST-AP(1)	M14 Surrogate Anti-Personnel Mine, made from 5.2 cm diameter plastic pipe 4.2 cm high, filled with paraffin wax and some small metal parts.	Not critical, target symmetric
ST-AP(2)	PMN Surrogate Anti-Personnel Mine, made from 11.8 cm diameter plastic pipe 5 cm high, filled with paraffin wax and some small metal parts	Trigger mechanism of the target perpendicular to the direction of sweep
ST-AP(3)	PMN2 Surrogate Anti-Personnel Mine, made from 11.5 cm plastic pipe 5.3 cm high, filled with paraffin wax and some small metal parts	Trigger mechanism of the target perpendicular the direction to of sweep

Table 1: Targets used in the experiments.

Targets were buried in dry sand approximately 0.5 cm deep. The antenna was hung from a track along which it could be driven at constant velocity by a stepper-motor at a height of approximately 0.5 cm above the surface of the sand (see Figure 1). Each target was placed such that the antenna would cross its centre. The antenna was oriented so that the transmitter crossed the target first, followed by the receiver and, in both cases, the antenna electric polarisation was perpendicular to the direction of travel. This results in the most complex target image and highlights the internal structure of the targets. The antenna size and separation is of the order of the size of the targets. The velocity of the antenna was adjusted to give soundings 0.1 cm apart and each measurement set comprised approximately 1200 backscattered GPR soundings. These measurements were initiated and terminated well off the target so that a large amount of data was available with no target present. The time range of the GPR soundings was 6 ns which corresponds to a sampling interval of $\Delta t = 0.0117$ ns.

Shallow-target GPR soundings measured using a bistatic polar antenna are normally obscured by the antenna cross-coupling and surface return. These effects are considered to be approximately constant over a number of soundings and may be crudely removed by a process called background subtraction. In this process, the average of N_b neighbouring echoes over a small area with no target present is usually subtracted from the time domain soundings with the target present. An example of the GPR backscattered signals recorded in sand across the surrogate landmine ST-AP(2) is shown in Figure 2. Figure 2 (a) shows the raw measured signatures. Figure 2 (b) shows the GPR signatures processed using background removal with $N_b = 1$. The position of the target is clearly visible in this

image.

The data files used our in experiments are listed in Appendix B.

4 Results and Discussion

To demonstrate the performance of the KT algorithm we first apply it to modelling a simulated signal composed of two exponentially damped sinusoids in noise. The complex conjugate poles of this signal are $s_{1/2} = -0.02 \pm j0.18$ and $s_{3/4} = -0.01 \pm j0.1$, and the corresponding amplitudes are $C_{1/2} = 2000 \pm j3$ and $C_{3/4} = 100 \pm j3000$. The order of the model is $M = 4$. The signal is contaminated by additive zero-mean white Gaussian noise with variance $2\sigma^2$. Peak signal-to-noise ratio (SNR) used in this example is set to 15 dB. This simulated signal contaminated by noise is shown in Figure 3.

The KT algorithm was applied to model this noise contaminated signal with the order of the backward linear prediction equations in Eq.(2) set to $L = 50$. Two approaches described in Section 2.2 were used to determine the order of the model M. The information-theoretic method [28] predicted $\hat{M} = 6$, whereas simple thresholding of the singular values of the data matrix determined the order as $\hat{M} = 38$, where the parameter t was set to 0.050. That is, in this case, when the data are truly derived from a finite order autoregressive (AR) model, very good estimate of the model order M was obtained by using the information-theoretic criterion, as compared to the simple thresholding of the resulting singular values. However, as will be seen below, the information-theoretic approach usually does not perform as well when the data model is not exact, *i.e.*, when it is used with the real signals [25].

The zeros of the prediction error filter polynomial $B(z)$ computed for the simulated signal using the KT algorithm and the information-theoretic criterion for the model selection are shown in Figure 4. The four signal zeros that fall outside the unit circle are clearly visible, whereas the extraneous zeros are within the unit circle.

The approximated signal obtained by modelling the noise contaminated data in Figure 3 using the KT algorithm along with the original (noiseless) data is shown in Figure 5 (a). For comparison, Figure 5 (b) shows the signal obtained by modelling the same data using the Prony method. The parameters of the Prony method were: the order of the model $M = 6$, the spacing (stride) $k = 10$ and no signal sub-sampling has been applied (see [15] for more details on the parameters of the Prony algorithm). Table 2 presents the true and the estimated signal poles obtained by using the KT and the Prony algorithms.

The parameters of the Prony algorithm, M and k, used in this example are those for which the resulting estimated poles and residues were closest to their true values. For other combinations of M and k the obtained estimates were much worse. The intention was to keep the parameter M as close as possible to its true value and to obtain, at the same time, good estimates of poles and residues. As can be seen from Table 2 for the above parameters two real poles and two pairs of complex-conjugate poles were obtained using the Prony method. We consider real poles as spurious and not really important and treat the conjugate-complex poles as our result. It is interesting to note that when the order of the model was set to $M = 4$ only two complex-conjugate poles resulted,

SIMULATION RESULTS

True poles	Estimated poles	
	KT	Prony
-0.02 ±j0.18 -0.01 ± j0.10	-0.0196 ± j0.1796 -0.0079 ± j0.1007	0.0036 ± j0.1946 -0.098 ± j0.0916 0.019 -0.0016
True residues	**Estimated residues**	
	KT	**Prony**
2000 ± j3 100 ± j3000	2158.8 ± j45.9 193.6 ± j2596.5	100.3 ± j137.9 -879.1 ± j2722.6 -8.9 227.6

Table 2: The true parameters of the simulated signal and the parameters estimated using the KT and the Prony algorithms.

along with two spurious real poles. We also mention that the estimates obtained by using the Prony method change randomly when the parameters M and k are changing, and, though it may be possible to get an estimate as good as the one shown in Figure 5 (b), the associated search procedure is usually long and painstaking. In comparison the KT algorithm is much more robust and outperforms the Prony method when applied to this highly contaminated data.

The programs for modelling the GPR signatures using the KT algorithm and the Prony approach are implemented using Matlab Numeric Computation and Visualisation Software. These programs are listed in Appendix C.

We now use the KT algorithm to estimate the model parameters of the backscattered GPR echoes corresponding to the targets presented in Table 1. Since the GPR [29] is designed in such a way that its soundings are over-sampled, we first sub-sample these signals by using the appropriate low-pass filter and decimating them by a factor $S = 2$ ($S = 3$ gives very similar results). It has been observed that more exact pole estimates are obtained when the signal is sub-sampled in this way. The reason is that most of the energy of the originally acquired signal is concentrated in the lower part of the spectrum, and, by filtering and decimating the signal in this way, useful and interesting part of the spectrum is distributed fully around the unit circle and is not restricted to a small angular interval. This is desirable, since the resolution of the signal poles is increased and their more accurate estimation by the KT algorithm is enabled.

Increasingly better signal fits are obtained as the order of the model M increases. In this case, however, the estimated signal poles tend to be more and more dispersed. For this reason our intention was to choose the minimum M for which the signal is still reasonably well approximated. When applied to the real data, the model selection based on thresholding the singular values of the data matrix gave much better results compared to the information-theoretic criteria. Examples of modelling the GPR signals reflected from the surrogate landmines ST-AP(2) and ST-AP(3) using the KT algorithm and the method

based on thresholding the singular values of the data matrix are shown in Figures 6 and 7, respectively, where $L = 90$ (note that these are raw GPR signatures, *i.e.*, without background removal). The thresholding method resulted in $\hat{M} = 10$ and $\hat{M} = 12$ for these two targets for $t = 0.025$. From Figures 6 and 7 it can be seen that the approximated signals obtained by using the above model orders were very good. In contrast, the information-theoretic criteria [28] gave $\hat{M} = 88$ for ST-AP(2) and $\hat{M} = 90$ for ST-AP(3) which were obviously too big. For these reasons, in this report we exclusively applied the thresholding method to determine M for modelling the measured signatures of our targets.

The models estimated using the thresholding technique were in most cases insensitive to changing the parameter t within a range of values. For example, for the above signals, where we set $t = 0.025$, this range was from 0.010 to 0.040, approximately. This stability of the model estimates for varying values of t within a given range was used as a confirmation that the value of the parameter ($t = 0.025$ in this case) was appropriately chosen.

In order to fully characterise each target the signal poles are computed using a series of neighbouring signatures recorded over each target type. The poles estimated from neighbouring signatures are similar but not necessarily the same. The number of poles may also vary from one signal to the other. This spatial variation of signal poles can be caused by the internal structure of the target, the characteristics of the imaging system (size of the target vs. the distance between the transmit and receive antennas), the influence of noise, etc.

The poles computed for the targets in Table 1 are projected in two-dimensional α-f plane (see Figures 8 and 9). Figure 8 (a) shows the poles corresponding to the three surrogate landmines and Figure 8 (b) shows the poles computed for the three PVC cylinders where the raw target signatures were used for modelling. The poles corresponding to different target-types form clusters in the α-f space. It is expected that the positions of such clusters, which are clearly marked in Figures 8 (a) and (b), can be used for target identification. For comparison, Figure 10 shows the poles computed from the (neighbouring) backscattered GPR echoes corresponding to the case of no target present (*i.e.*, the background signals).

Since the GPR signals are obscured by the clutter it is also reasonable to apply the background removal technique as explained in Section 3 to compute the target signatures. An important question is how to choose the particular no-target-present signals to be subtracted. In our experiments the signals to be subtracted from the raw target echoes are chosen randomly from the background signals within the target-specific measurement sets. This process is repeated for each target-type separately. Figures 9 (a) and (b) show the poles resulted from modelling such background removed signals corresponding to the surrogate landmines and the PVC cylinder, respectively. It can be seen that, though the poles of the background-removed signals corresponding to different targets still form a number of non-overlapping and partially overlapping clusters, they are also more dispersed as compared to the poles computed from the raw signatures (Figures 8 (a) and (b)). This effect is expected since the background subtraction process effectively decreases the SNR of the modelled signals. For this reason the parameter t in the method for the model order estimation was set to $t = 0.080$ for modelling the background-removed signatures, as opposed to the value of $t = 0.025$ which was used when the raw target signatures were approximated.

The ground and target returns comprising the GPR signal can have different time shifts with respect to the beginning of the measurement (*i.e.*, sampling). This time shift can be adjusted on the GPR system at the time when the measurements are taken, so as to take into account the measurement conditions, such height of the GPR over the ground, etc. If the ground surface is relatively flat all signatures comprising one measurement set will have similar time shifts. This shift may vary from one measurement set to the other. Since the modelling technique we apply is, in general, not shift invariant, the estimated poles usually change as the time shift changes. To be able to compare the poles extracted from the signatures that belong to different files, the modelled signals should be aligned so as to have the same reference point. An investigation is needed into the approaches for defining this starting point automatically in a consistent manner for various types of signatures.

To compute the target poles in the experiments described in this report we used the portion of the original 512-samples-long GPR soundings comprising the samples from $N_{beg} = 20$ to $N_{end} = 400$. Here the reference point N_{beg} was the same for all data files since in our experiments all measurement sets have been taken so as to have the same time shift. Samples from $N = 401$ to $N = 512$ have been discarded since they do not contain any significant signal variation.

The position of the target in a set of measurement is determined by visual inspection (see Figure 2). This process can also be automated, since the variances of the GPR echoes reflected from the target are substantially bigger than those corresponding to the background signals, in particular when the background-subtracted signatures are used. Consequently, a statistical test based on the variance of the signal might be applied to determine whether there is a target present, and then poles would be extracted from these signals. It is expected that the feasibility of this and related approaches will be examined in some detail in the future.

5 Conclusions and Recommendations

We have investigated an approach to modelling the backscattered GPR echoes from various types of buried non-metallic-cased surrogate landmines and PVC cylinders using the KT algorithm. Both raw and background-removed target signatures have been considered. It has been shown that the poles extracted in this way form clusters which are characteristic of a given target-type. Consequently, it is expected that such poles can be used for the recognition of landmines.

The KT algorithm has been applied to synthetic data contaminated by white Gaussian noise and to experimental data. In modelling the synthetic signal the performance of the KT method has been compared to the Prony algorithm as applied in [15] with more stable results.

Two different approaches for selecting the order of the model for the KT algorithm have been investigated: an information-theoretic and an approach based on the thresholding of singular values of the data matrix. While the information-theoretic criterion was successful for the simulated data which were computed using the the exact signal model, the simpler thresholding approach performed better when applied to the real data. The

poles computed using the KT algorithm and this latter approach were stable for a range of threshold values.

The results presented in this report correspond to only one soil type (dry sand) where the signals were measured using 1.4 GHz antenna. It is well known that propagation of electromagnetic waves depends on the properties of the medium, and we can expect to obtain different results for the soil types with varying dielectric constants. For example, higher dielectric constants introduce higher losses, so the returned signal is weaker. The dielectric constants also increase with the moisture content of the soil. It remains to be seen how different conditions, *i.e.*, soil types, depths at which the target is buried, different target aspects, etc., affect the pole estimates, and, what antenna bandwidths provide most information for the recognition. The use of balanced bridge antennas should also be considered.

Further research is needed to determine whether or not to use the background-removed signatures, and how to define the background signal to be subtracted. A viable approach to this problem would be to use the assumption that, when the raw target signatures are modelled, some of the resulting poles correspond to the antenna cross-coupling and ground return, whereas other poles represent the part of the signal returned from our target. Therefore, the background signal might be synthetised for each signature using the poles corresponding to the ground return. These synthetised background signals would then be subtracted from the raw signals. In this way some of the poles originally obscured by the clutter could be extracted. It is expected that detection/recognition of small targets could be improved in this way.

We are also looking into developing a pattern recognition system for buried targets based on the pole estimates and we will be fusing this information with the signals obtained from a metal detector.

Following is the summary of our recommendations for the future work on detection/recognition of landmines:

- It is necessary to investigate target signatures for various soil types and conditions to determine the stability of poles.
- Signals recorded using different centre frequency antennas need to be examined to determine the frequency range optimal for detection and identification of landmines.
- It is important to undertake further research on choosing the most suitable background removal method. In addition, approaches to determining, in a consistent manner, the part of the original 512-samples-long GPR soundings to be used in the KT modelling for a range of targets and environment conditions, need to be investigated.
- Techniques for target detection using the signal variance and other approaches need to be investigated in order to locate the target.
- Since the GPR has difficulty discriminating between the small targets and clutter, it is envisaged that much better identification results could be obtained by fusing the information obtained from the EMI metal detector and that from the GPR alone.

- In parallel with the above it is necessary to define the most appropriate pattern recognition method for landmine identification based on the estimated poles.

References

1. D. J. Daniels, D. J. Gunton, and H. F. Scott. Introduction to subsurface radar. *Proc. IEE*, 135 (F)(4):278–317, 1988.

2. D. J. Daniels. *Surface penetrating radar.* Radar, sonar, navigation and avionics series 6. The Institution of Engineers, London, UK, 1996.

3. C. E. Baum, E. J. Rothwell, K.-M. Chen, and D. P. Nyquist. The singularity expansion method and its appliaction to target id entification. *Proc. IEEE*, 79(10):1481–1491, October 1991.

4. L. C. Chen, D. L. Moffatt, and L. Peters Jn. A characterization of subsurface radar targets. *Proc. IEEE*, 67(7):951–1000, July 1979.

5. L. C. Chan, L. Peters Jr., and D. L. Moffatt. Improved performance off a subsurface radar target identification system through antenna design. *IEEE Trans. Antenna Propag.*, 29(2):307–311, March 1981.

6. E. M. Kennaugh. The K-pulse concept. *IEEE Trans. Antennas Propag.*, 29(2):327–331, March 1981.

7. K.-M. Chen, D. P. Nyquist, E. J. Rothwell, L. L. Webb, and B. Drachman. Radar target discrimination by convolution of radar return with extinction-pulses and single-mode extraction signals. *IEEE Trans. Antennas Propag.*, 34(7):896–904, July 1986.

8. E. J. Rothwell, K.-M. Chen, and D. P. Nyquist. Extraction of natural frequencies of a radar target from a measured response using E-pulse. *IEEE Trans. Antennas Propag.*, 35(6):715–720, June 1987.

9. Y. Bissessur and R. N. G. Naguib. Buried plant detection: A Volterra series modelling approach using atrificial neural networks. *Neural Networks*, 9(6):1045–1060, 1995.

10. J. W. Brooks and M. W. Maier. Applicatiion of system identification and neural networks to classification of land mines. In *Proc. EUREL Int. Conf., 7-9 Oct. 1996, EICC, Edinburgh, UK*, pages 46–50, 1996.

11. H. C. Strifos, K.-M. Chen, S. Abramson, B. Brusmark, and G. C. Gaunaurd. Signature features in time-frequency of simple targets ectracted by ground penetrating radar. In *Proc. IEEE Intrnational Radar Conf., 8-11 May, Virginia*, 1995.

12. M. L. Blaricum and R. Mitra. A technique for extracting the poles and residues of a system directly from its transient response. *IEEE Trans. Antennas Propag.*, 23(6):777–781, November 1975.

13. M. L. Blaricum and R. Mitra. Problems and solutions associated with Prony's method for processing transient data. *IEEE Trans. Antennas Propag.*, 26(1):174–182, January 1978.

14. R. Kumaresan, D. W. Tufts, and L. L. Scharf. A Prony method for noisy data: chosing the signal components and selecting the order in exponential signal models. *Proc. IEEE*, 72(2):230–233, 1984.

15. D. Carevic, M. Craig, and I. Chant. Modelling GPR echoes from land mines using linear combinations of exponentially damped sinusoids. In *Proc. SPIE AeroSense '97, Orlando, USA*, April 1997.

16. R. Kumaresan and D. W. Tufts. Estimating the parameters of exponentially damped sinusiods and pole-zero modeling in noise. *IEEE Trans. Acoustic, Speech, Signal Proc.*, 30(6):833–840, 1982.

17. Y. Hua and T. K. Sarkar. Generalized pencil-of-function methods for extracting poles of an em system from its transit reponse. *IEEE Trans. Antennas Propag.*, 37(2):229–234, February 1989.

18. Y. Hua and T. K. Sarkar. Matrix pencil metod for estimating parameters of exponentially damped/undamped sinusiods in noise. *IEEE Trans. Acoustic, Speech, Signal Proc.*, 38(5):814–824, May 1990.

19. Y. Bresler and A. Macovski. Exact maximum likelihood parameter estimation of superimposed exponentioal signals in noise. *IEEE Trans. Acoustic, Speech, Signal Proc.*, 34(5):1081–1089, October 1986.

20. M. A. Rahman and K.-B. Yu. Total least squares approach for frequency estimation using linear prediction. *IEEE Trans. Acoustic, Speech, Signal Proc.*, 35(10):1440–1454, October 1987.

21. R. Carriere and R. L. Moses. High resolution radar target modeling using a modified Prony method. *IEEE Trans. Antennas Propag.*, 40(1):13–18, January 1992.

22. D. P. Ruiz, M. A. Carrion, A. Gallego, and A. Medouri. Parameter estimation of exponentially damped sinusiods using a higher order correlation-based approach. *IEEE Trans. Signal Proc.*, 43(11):2665–2667, November 1995.

23. P. Barone, E. Massaro, and A. Polichetti. The segmented Prony method for the analysis of non-stationary time series. *Astron. Astrophys.*, 209:435–444, 1989.

24. R. Kumaresan. On the zeros of the linear prediction-error filter for deterministic signals. *IEEE Trans. Acoustic, Speech, Signal Proc.*, 31(1):217–220, 1983.

25. C. W. Therrien. *Discrete random signals and statistical signal processing.* Prentice Hall, Englewood Cliffs, NJ 07632, 1992.

26. H. Akaike. A new look at the statistical identification. *IEEE Trans. Automat. Contr.*, 19:716–723, December 1974.

27. J. Rissanen. Modeling by shortest data description. *Automatica*, 14:465–471, 1978.

28. V. U. Reddy and L. S. Biradar. SVD-based information theoretic criteria for detection of the number of damped/undamped sinusoids and their performance analysis. *IEEE Trans. Signal Proc.*, 41(9):2872–2881, 1993.

29. W. Murray, Williams C, J, and J. T. A. Pollock. A high resolution radar for mine detection. In *Proc. EUREL Int. Conf., EICC*, Edinburgh, UK, 7-9 Oct. 1996.

30. B. B. Y. Wong, I. Chant, G. N. Crisp, K. Kappra, K. Strugess, A. Rye, and K. Sherbondy. Suggested soil characterisation techniques and surrogate targets for ultra-wideband radar mine detection experiments. In *Proc. SPIE AeroSense '97, Orlando, USA*, April 1997.

Appendix A
Figures

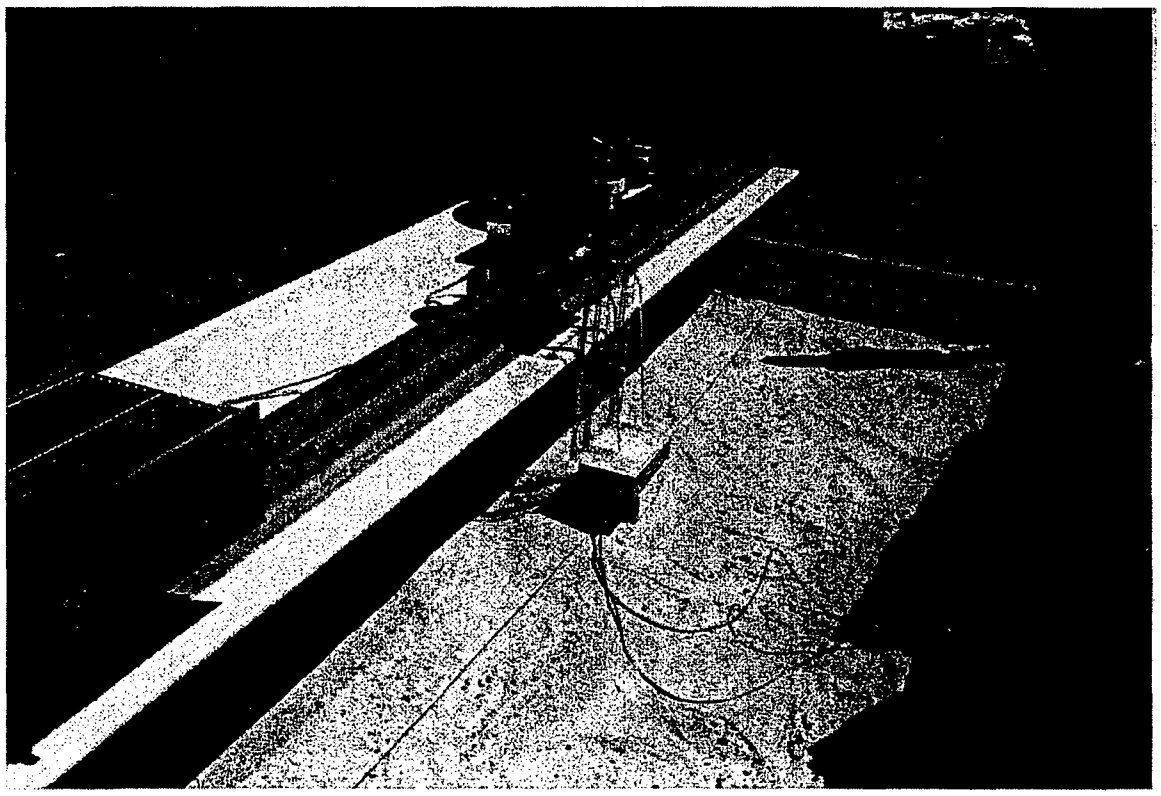

Figure 1: The GPR experiment in progress. Pictured is the antenna track sitting across the dry sand box with the GPR attached.

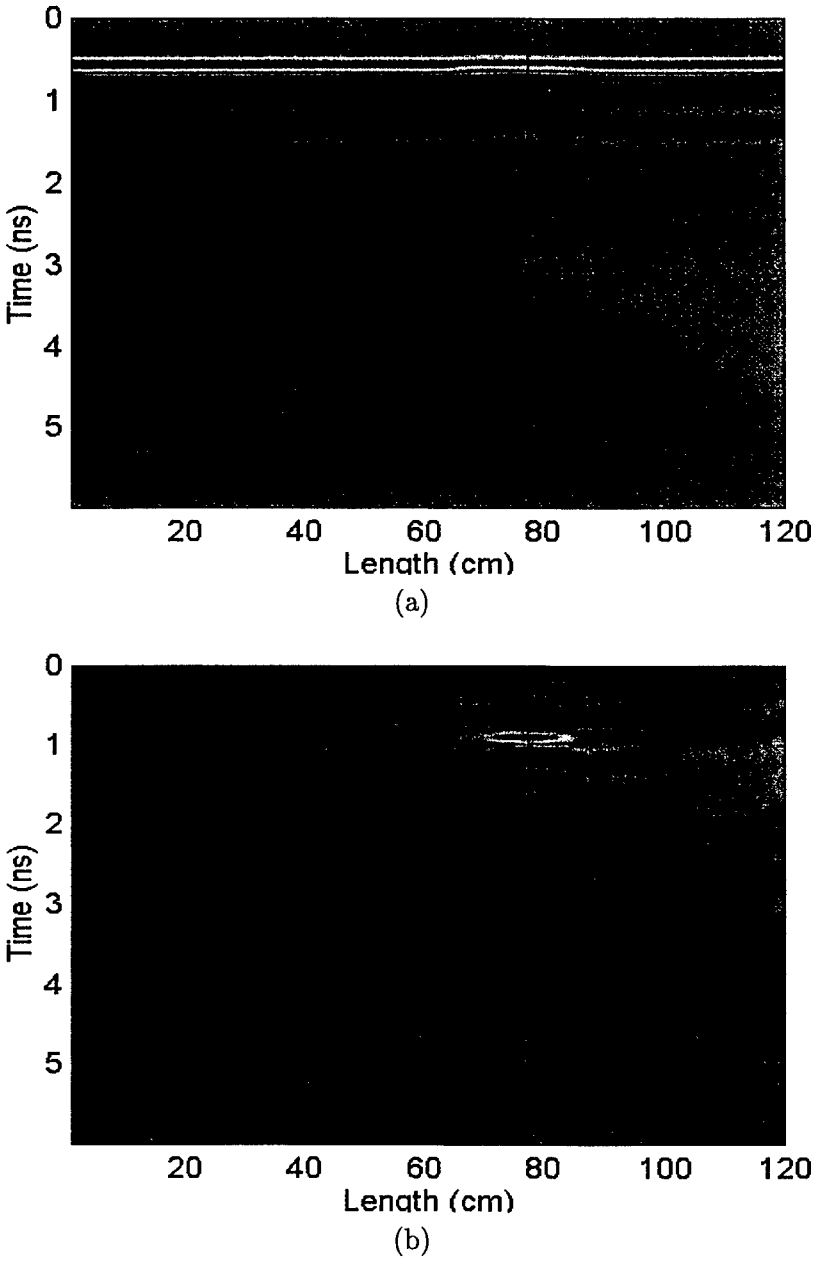

Figure 2: GPR backscattered signals taken in sand across the surrogate landmine target ST-AP(2). (a) original (raw-data) soundings; (b) background signal subtracted from the data. The position of the target in the image is indicated.

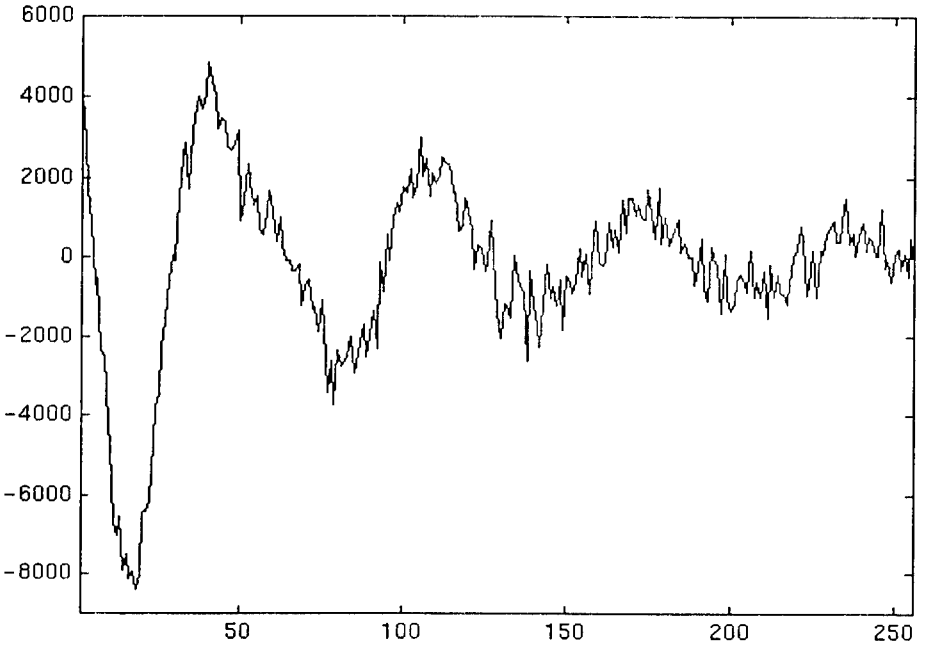

Figure 3: Noise contaminated simulated signal.

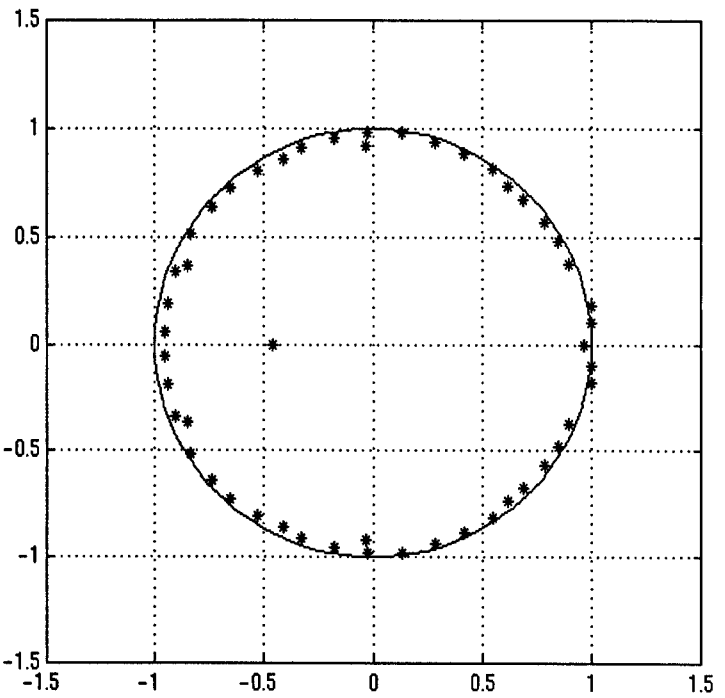

Figure 4: Zeros of the prediction-error filter polynomial $B(z)$. The signal poles are outside the unit circle whereas the extraneous zeros falls within the unit circle.

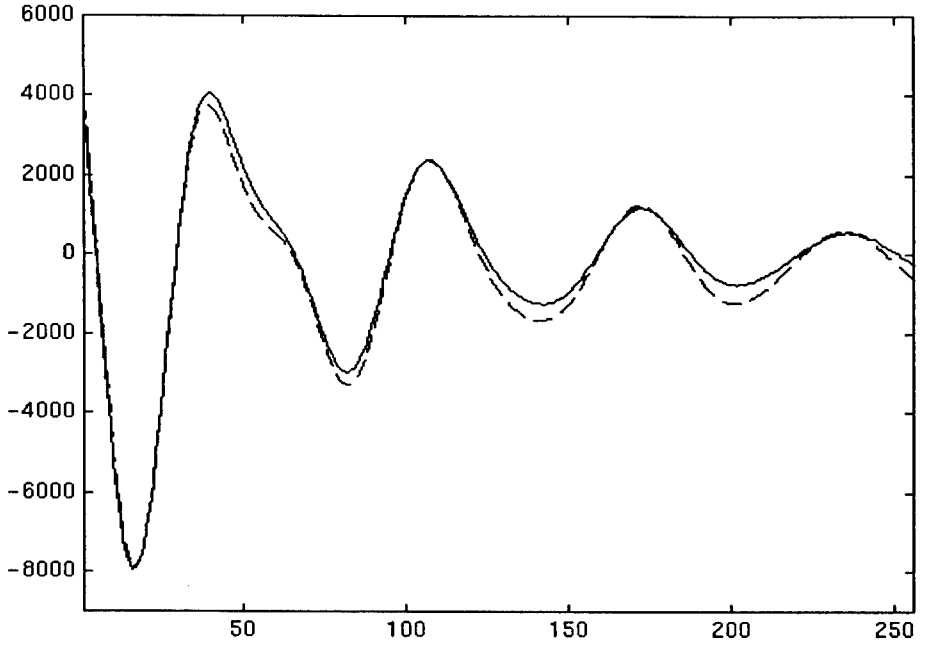

(a)

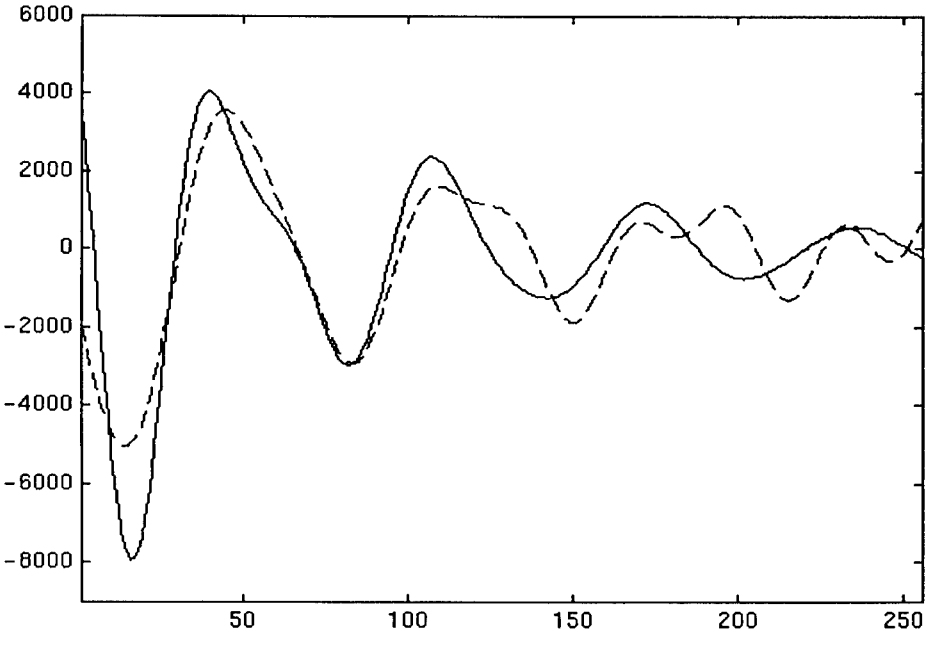

(b)

Figure 5: Modelling the simulated signal: noiseless signal (solid line) and the signal obtained by modelling the noisy data in Figure 3 using (a) KT algorithm (b) Prony algorithm.

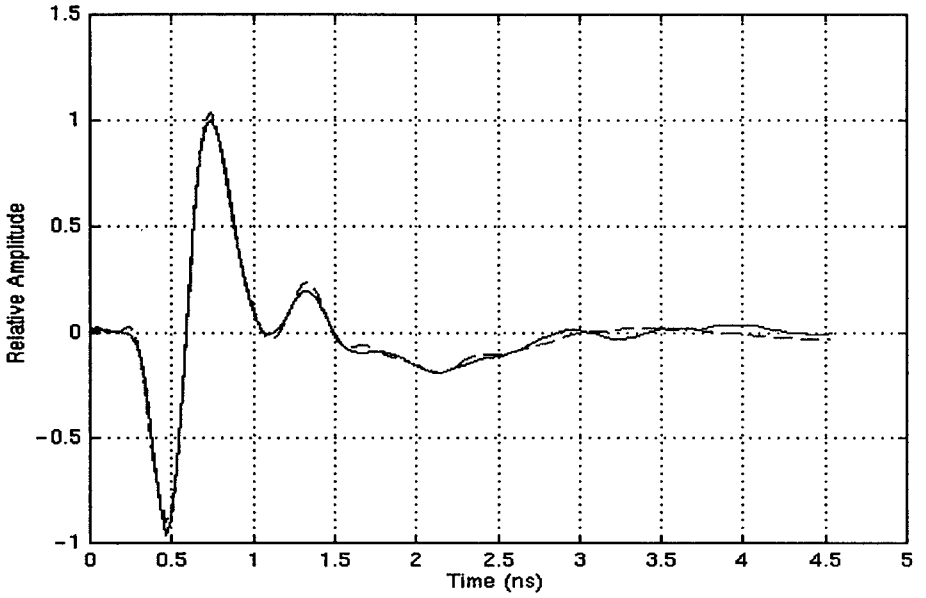

(a)

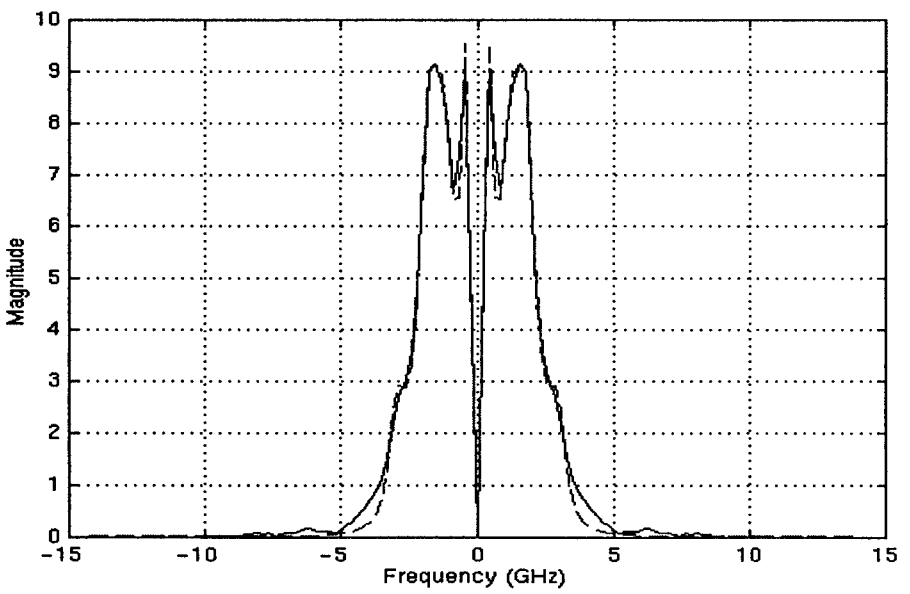

(b)

Figure 6: GPR signature of the surrogate land mine ST-AP(2): (a) time-domain representation (normalised to the values between 1 and -1); (b) frequency-domain representation. Solid line represents the original signature and dashed line corresponds to the signal modelled using the KT algorithm. The method based on the thresholding of the singular values of data matrix was applied to determine the model order with $t = 0.025$.

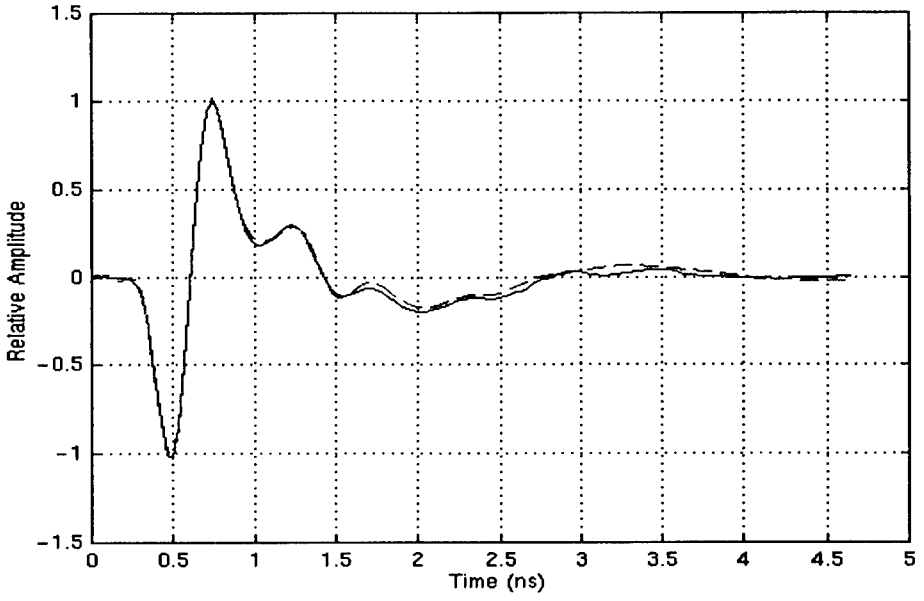

(a)

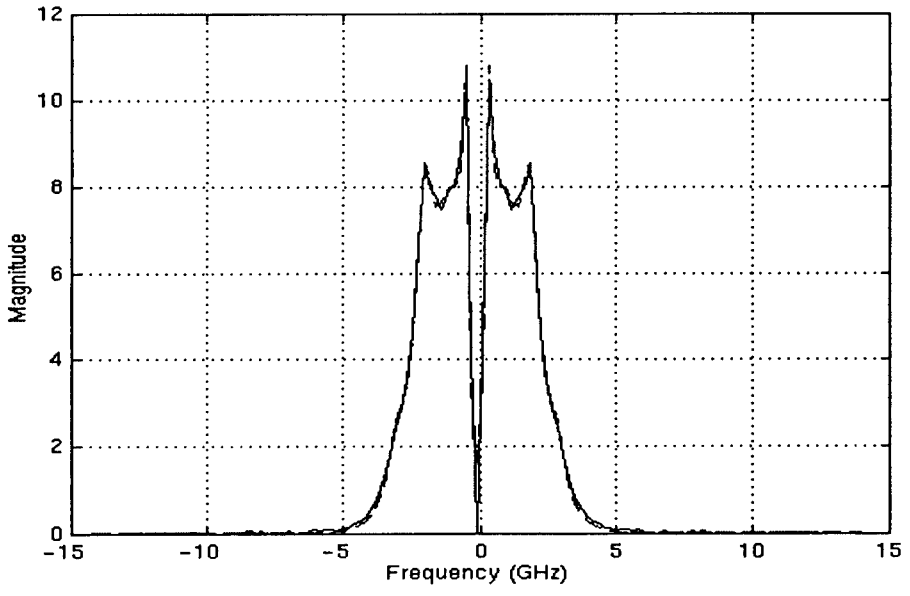

(b)

Figure 7: GPR signature of the surrogate land mine ST-AP(3): (a) time-domain representation (normalised to the values between 1 and -1); (b) frequency-domain representation. Solid line represents the original signature and dashed line corresponds to the signal modelled using the KT algorithm. The method based on the thresholding of the singular values of data matrix was applied to determine the model order with $t = 0.025$.

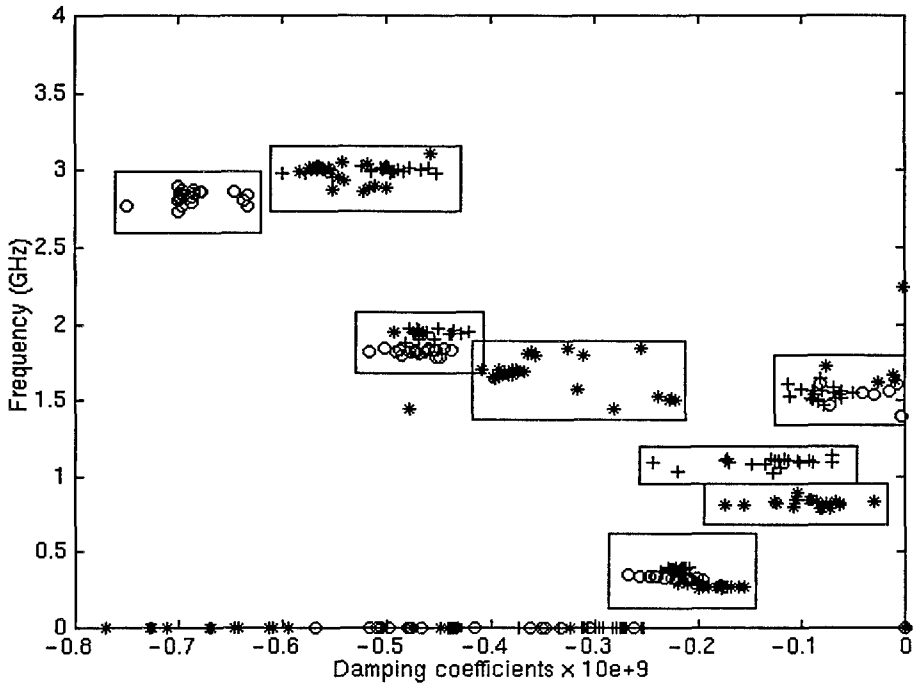

(a)

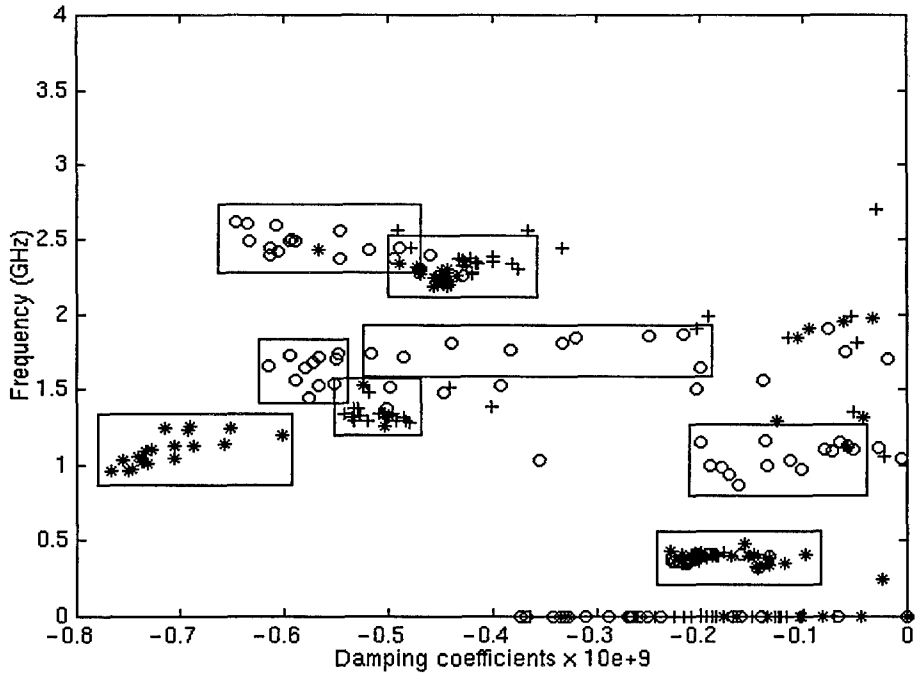

(b)

Figure 8: Poles of the raw GPR signatures corresponding to the test targets listed in Table 1 estimated using the KT algorithm with $L = 90$: (a) surrogate land mines: 'o' - ST-AP(1), '+' - ST-AP(2), '' - ST-AP(3); (b) PVC cylinders: 'o' - PVC Test Target 1, '*' - PVC Test Target 2, '+' - PVC Test Target 3. The method based on the thresholding of the singular values of data matrix was applied to determine the model order with $t = 0.025$.*

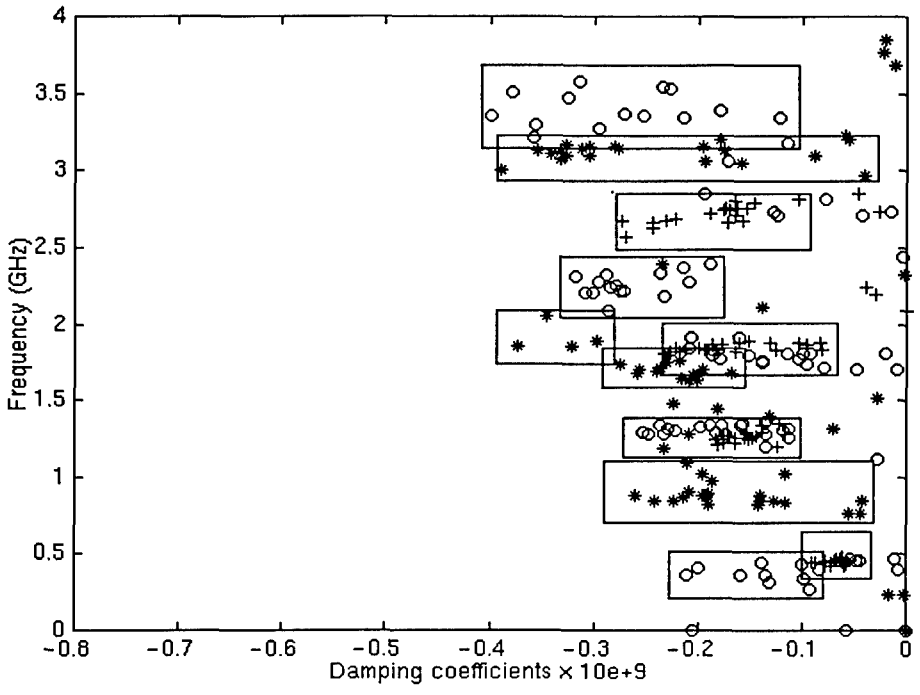

(a)

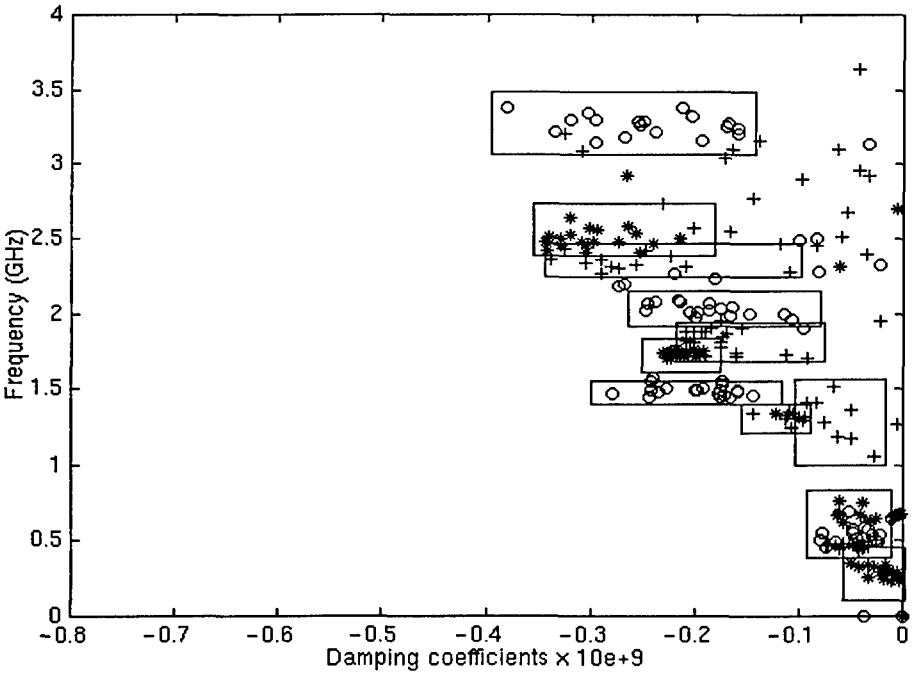

(b)

Figure 9: Poles of the background removed GPR signatures corresponding to the test targets listed in Table 1 estimated using the KT algorithm with $L = 90$: (a) surrogate land mines background subtracted: 'o' - ST-AP(1), '+' - ST-AP(2), '' - ST-AP(3); (b) PVC cylinders: 'o' - PVC Test Target 1, '*' - PVC Test Target 2, '+' - PVC Test Target 3. The method based on the thresholding of the singular values of data matrix was applied to determine the model order with $t = 0.080$.*

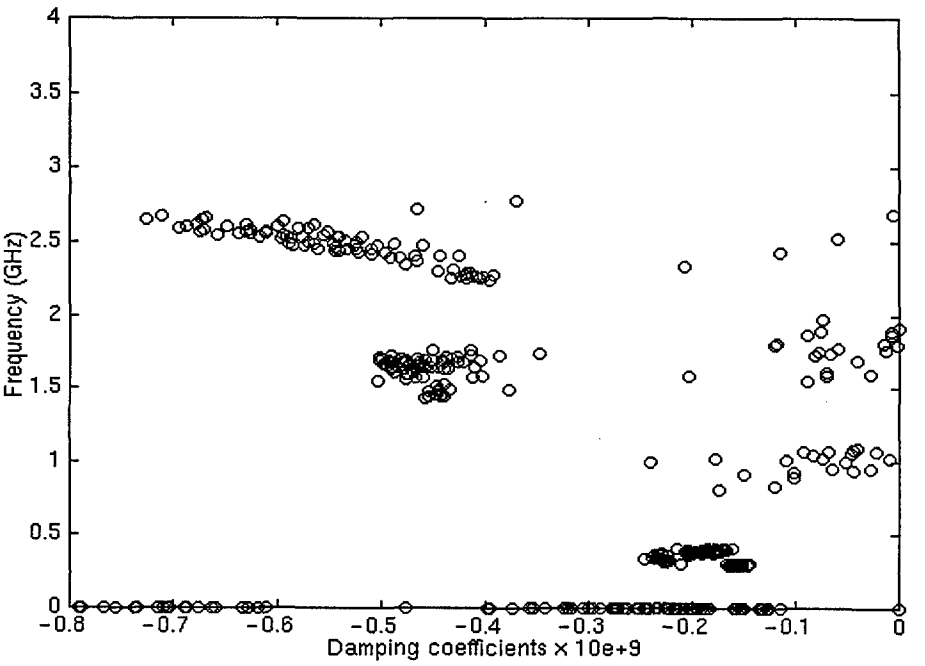

Figure 10: Poles of the GPR backscattered signals corresponding to the case of no target present (background signals) estimated using the KT algorithm with $L = 90$, The method based on the thresholding of the singular values of data matrix was applied to determine the model order with $t = 0.025$.

Appendix B
GPR Measurement Sets

Data files containing the measurements used in the experiments were obtained by FR-127-MSCB MK2 impulse GPR system. (Reference [29] provides detailed description of this GPR system.) The 1.4 GHz centre frequency antenna connected in non-differential mode was used and the soil was dry sand. The measurement procedure and the investigated targets are described in Section 3 of this report.

Table 3 shows the data files and the corresponding targets.

TARGET	FILE NAME
ST-AP(1)	/ANT141/SAND/SURR1/FILE1
ST-AP(2)	/ANT141/SAND/SURR3/FILE1
ST-AP(3)	/ANT141/SAND/SURR2/FILE1
PVC Test Target 1	/ANT141/SAND/PVCCYL1/FILE1
PVC Test Target 2	/ANT141/SAND/PVCCYL2/FILE1
PVC Test Target 3	/ANT141/SAND/PVCCYL3/FILE1

Table 3: GPR data files used in the experiments.

Appendix C
Program Listings

```
% ************************************************************************
*
%
%   Function:           [P,R,A]=ktalg(D,L,step,sc,fb,svdt)
%
%   Models the signal as a sum of exponetially damped sinusois using the
%   KT algorithm.
%
%
%   Input:    D - real matrix comprising  m GPR traces of length n
%                 (averaged to obtain a single trace)
%             L - maximum reqired number of poles
%             sc - if sc>1 data is low-pass filtered and correspondingly
%                  decimated. sc values: 2, 3, 4, etc.
%             fb   1 - forward prediction
%                 -1 -  backward prediction
%             step - required spacing between successive samples
%             svdt - parameter for thresholding the singular values
%                    of the data matrix
%
%  Output:    P - complex vector of dimension dim=30 containing signal
%                 poles and the following data: deg (dim), ste (dim-1),
%                 sc (dim-2) and fb (dim-3)
%             R - complex vector containing corresponding residues
%             A - real vector containing approximation of the input trace
%
%   Author:   Dragana Carevic
%             DSTO Tactical Surveillance Systems Division
%             tel: 8259 6804
%             email: dragana.carevic@dsto.defence.gov.au
%   Date:     6/4/1997
%
%
%                Kumaresan and Tufts algorithm explained in:
%
%                R. Kumaresan and D. W. Tufts
%                " Estimating the parameters of  exponentially damped sinusiods
%                and pole-zero modeling in noise, " IEEE Trans. Acoustic,
%                Speech, Signal Proc. pp. 833-840, 1982.
%
%                SVD based information-theoretic criteria for order selection
%                as per:
```

```
%                V. U. Reddy and L. S. Biradar
%                " SVD-based information theoretic criteria for detection
%                of the number of dumped/undumped sinusiods and their
%                performance analysis," IEEE Trans Sig. Process. Vol. 41
%                No. 9, September 1993.
%
%   Uses:  reconst.m
%
% ***************************************************************************


              function [P,R,A] = ktalg(D,L,step,sc,fb,svdt);


[n,m]=size(D);
[MM,beg]=max(D);

if m>1
   fp=mean(D(:,1:m)')';
   m=1;
else
   fp=D;
end;

% Low-pass filtering and decimation if sc>1
if sc>1
  lh=50; %length of the low-pass fir filter
  f=decimatf(fp,sc,lh,'fir');
  [n,l]=size(f);
else
  f=fp;
end;
clear fp;

ave=mean(f);
f=f-ave;

% Start here
dim=30;
P=zeros(dim,1);
R=zeros(dim,1);
A=zeros(n,1);
n1=n-step*L

%  Compute data matrix FP
if fb==1          %FORWARD PREDICTION
fprintf('Forward\n');
```

```
for k=1:(n1)
  t=k:step:((L-1)*step+k);
  FP(k,:)=f(t)';
  y(k)=f(L*step+k);
end;
elseif fb==-1   %BACKWARD PREDICTION
fprintf('Backward\n');
for k=1:n1
  t=k+step:step:L*step+k;
  FP(k,:)=f(t)';
  y(k)=f(k);
end;
end;

%  Compute singular value decomposition of FP
[U,S,V]=svd(FP);
S(1:L/2,1:L/2);
J=diag(S);


%  Apply SVD-based information-theoretic criteria for
%  detecting the number of poles

h=U'*y'; HN=norm(h,2)^2;
r=n1;
for k=1:L/2
 HN=HN-(h(2*k-1))^2-(h(2*k))^2;
 sum=r*(1+log(2*pi)+log(HN/r));
 AIC(k,1)=sum+2*(2*k+1);
 MDL(k,1)=sum+(2*k+1)*log(r);
end;

[mmin,k]=min([AIC,MDL]);
[m,k1]=min(mmin); M1=2*k(k1);
fprintf('Information-theoretic model order is %d\n',M1);

%  A heuristic criterion for determining model order
for k=3:L
    if S(k,k)<svdt*S(1,1) % 0.025 for sc=2 and raw signal ant 1.4 GHz
                          % 0.050 for sc=2 and background removed data 1.4 GHz
                          % 0.050 fo sc=2, raw data 3GHz
    break;
  end;
end;
if rem(k,2)==0
  M2=k;
else
```

```
  M2=k-1;
end;

fprintf('Heuristic model order is %d\n',M2);

% Compute vector b
M=M2;
S=diag(S);
S=diag(ones(M,1)./S(1:M));
b=zeros(L,1);
b=-V(:,1:M)*S*U(:,1:M)'*y';

PC=zeros(L+1,1);
PC(1,1)=1; PC(2:L+1,1)=b;

% Solve characteristic equation
RTS=roots((PC));
% Plot roots on the unit circle
     %figure;plot(RTS,'*');grid;
     %hold on; % plot unit circle
     %w=0:2*pi/100:2*pi;
     %a=cos(w)+j*sin(w);
     %plot(imag(a),real(a));
     %axis([-1.5,1.5,-1.5,1.5]);

% Choose poles which fall outside unit circle
ist=1/step;
if fb==-1
  i=find(abs(RTS)>1);
  [K1,K2]=size(i);
  K=K1; if K1==1
          K=K2 %this is final number of poles
        end;

for k=1:K
 P(k,1)=-ist*log(RTS(i(k)));
 if abs(imag(P(k)))*step==pi
  P(k,1)=real(P(k,1));
end;
end;
else
  P(1:L,1)=ist.*log(RTS);K=L;
end;

RTS=RTS(i);clear i;
[Y,i]=sort(abs(imag(P(1:K,1))));
PS=zeros(dim,1);
```

```
PS(1:K,1)=(P(i));
P(dim,1)=K;
P(dim-1,1)=step;
P(dim-2,1)=sc;
P(dim-3,1)=fb;
PS(dim-3:dim,1)=P(dim-3:dim,1);
P=PS;
deg=K;



% Compute the residuals and signal approximation

[res,a]=reconst(f,P);


R(1:deg)=res;   %residuals

A=a+ave;
        % aproximate signal
fo=f+ave;
       % input signal

% Plot the reconstructed signal in time and frequency domains

TB=6; % time base in nanoseconds 6 for 1.4 GHz antenna
      % 10 for 3.0 GHZ antenna
TP30=sc*TB/512; %in ns
FP30=1/TP30;    %in GHZ

 tt=(0:TP30:(n-1)*TP30);mmax=max(fo);
 fo=fo/mmax;A1=A/mmax;
 figure; plot(tt,fo,'b-'); grid;
 hold on; plot(tt,A1,'r--');hold off;
 xlabel('Time (ns)'); ylabel('Relative Amplitude');


 four(:,1)=10*log10(fftshift(abs(fft(fo))));
 four(:,2)=10*log10(fftshift(abs(fft(A1))));
 ff=(-FP30/2:FP30/n:(n-1)*FP30/(2*n));
 figure;plot(ff,four(:,1), 'b-');grid;
 hold on; plot(ff,four(:,2),'r--'); hold off;
 xlabel ('Frequency (GHz)'); ylabel('Magnitude (dB)');

end;    % function
```

```
%*************************************************************************
%
%   Function:           [P,R,A]=pronalg(D,L,step,sc)
%
%         Models the signal as a sum of exponetially damped sinusoids
%         using Prony method. Prony signal modelling involves computing
%         poles using principle component analysis.
%
%
%   Input:    D - real matrix comprising  m GPR traces of length n
%                 (averaged to obatin a single trace)
%             L - reqired number of poles
%             sc - if sc>1 data is low-pass filtered and correspondingly
%                  decimated
%             step - required spacing between successive samples
%   Output:   P - complex vector of dimension dim=30, containing signal
%                 poles and the following data: L (dim), step (dim-1)
%                 and sc (dim-2)
%             R - complex vector containing corresponding residues
%             A - real vector containing approximation the input trace
%
%   Author:   Dragana Carevic
%             DSTO Tactical Surveillance Systems Division
%             tel: 8259 6804
%             email: dragana.carevic@dsto.defence.gov.au
%   Date:     6/4/1997
%
%   Description: Input signal undergoes 'pole-zero' analysis and is
%                approximated using a constant offset term and several
%                damped sinusoidal oscillations, each treated as a pair
%                of conjugate complex exponetials.
%
%                On output poles x+iy and residues u+iv describe a conjugate
%                pair of model terms
%
%                        (u+iv)exp[(x+iy)t] and (u-iv)exp[(x-iy)t].
%
%                Predicted curves according to this model are returned in
%                a real matrix A.
%
% *************************************************************************


                    function [P,R,A] = pronalg(D,L,step,sc);


[n,m]=size(D);
```

```
[MM,beg]=max(D);

if m>1
   fp=mean(D(:,1:m)')';
   m=1;
else
   fp=D;
end;

%  Low-pass filtering and decimation if sc>1
if sc>1
  lh=50; %length of the low-pass fir filter
  f=decimatf(fp,sc,lh,'fir');
  [n,l]=size(f);
else
  f=fp;
end;
clear fp;

ave=mean(f);
f=f-ave;

%  Start here
dim=30;
P=zeros(dim,1);
R=zeros(dim,1);
A=zeros(n,1);
n1=n-step*L


%  Eigenvector solution
for k=1:(n1)
  t=k:step:((L-1)*step+k);
  FP(k,:)=f(t)';
  y(k)=f(L*step+k);
end;
FPP(:,1)=y'; FPP(:,2:L+1)=FP;

cov=FPP'*FPP./n1;
[VEC,D]=eig(cov);
incom=zeros(L+1,1);
for k=1:L+1
 incom(k,1)=D(k,k);
end;
[l,I]=sort(incom);
 I=reverse(I);
PC=VEC(:,I(L+1));
```

```
% Solve characteristic equation
RTS=roots((PC));

% Plot root and the unit circle
  % figure;plot(RTS,'k*');grid;
  % hold on; % plot unit circle
  % w=0:2*pi/100:2*pi;
  % a=cos(w)+j*sin(w);
  % plot(imag(a),real(a),'k');
  % axis([-1.5,1.5,-1.5,1.5]);

% Compute signal poles
ist=1/step;
for k=1:L
  if imag(RTS(k))==0
    P(k,1)=sign(RTS(k))*ist*log(abs(RTS(k)));
  else
    P(k,1)=ist.*log(RTS(k));
  end;
  end;
K=L;

[Y,i]=sort(abs(imag(P(1:K,1))));
PS=zeros(dim,1);
PS(1:K,1)=(P(i));
PS(dim,1)=K;
PS(dim-1,1)=step;
PS(dim-2,1)=sc;
P=PS;


% Compute residuals and signal approximation

[res,a]=reconst(f,P);

deg=K;

R(1:deg)=res;   % residuals

A=a+ave;
        % approximated signal

fo=f+ave;
       % input signal

% Plot the reconstructed signal in time and frequency domains
```

```
A=a+ave;
fo=f+ave;
TB=6; % time base in nano seconds 6 for 1.4 GHz antenna
      %  10 for 3.0 GHZ antenna
TP30=sc*TB/512; %in ns
FP30=1/TP30; %in GHZ

tt=(0:TP30:(n-1)*TP30);mmax=max(fo);
fo=fo/mmax;A1=A/mmax;
figure; plot(tt,fo,'b-'); grid;
hold on; plot(tt,A1,'r--');hold off;
xlabel('Time (ns)'); ylabel('Relative Amplitude');

four(:,1)=10*log10(fftshift(abs(fft(fo))));
four(:,2)=10*log10(fftshift(abs(fft(A1))));
ff=(-FP30/2:FP30/n:(n-1)*FP30/(2*n));
 figure;plot(ff,four(:,1), 'b-');grid;
 hold on; plot(ff,four(:,2),'r--'); hold off;
 xlabel ('Frequency (GHz)'); ylabel('Magnitude (dB)');


end;    % function
```

```
% ************************************************************************
%
%   Function:           [res,a]=reconst(f,pol)
%
%            Uses the computed poles to compute the residues and the
%            model-based approximation of the signal.
%
%   Input:   f - input signal of length n
%            P - complex vector of dimension dim=60, containing signal
%                poles  and the following data:
%                deg (i=dim), h (i=dim-1).
%  Output:   res - complex vector containing corresponding resid
%            a   - real vector containing approximation of the input
%                  signal f
%
%   Author:  Dragana Carevic
%            DSTO Tactical Surveillance Systems Division
%            tel: 8259 6804
%            email: dragana.carevic@dsto.defence.gov.au
%   Date:    20/4/1997
%
% ************************************************************************


              function [res,a] = reconst(f,pol);


[d,m]=size(pol); % d is the number of poles, m=1
deg=pol(d);
step=pol(d-1);
[n,l]=size(f);
a=zeros(n,1);

C=zeros(n,deg);
for k=1:n
  l=1; dt=1;
  while(l<=deg)
    r=real(pol(l)); w=imag(pol(l));
    C(k,l)=exp(r*k*dt)*cos(w*k*dt);
    l=l+1;
    if (w~=0)
     C(k,l)=-exp(r*k*dt)*sin(w*k*dt);
     l=l+1;
    end; %if
  end;   % while
end;    % k loop
```

```
X=inv(C'*C)*C'*f;  % LSE solution of CX=f
clear C;

res=zeros(deg,1);
l=1;
while(l<=deg)
  if imag(pol(l))==0 %real pole
   res(l)=X(l);
   l=l+1;
  else
   res(l)=X(l)./2+X(l+1)./2*j; % conjugate complex amplitudes
   res(l+1)=X(l)./2-X(l+1)./2*j;
   l=l+2;
  end; %if
end;   % while
clear X;

% Compute the reconstructed signal
a=zeros(n,1);
for k=1:n
  for l=1:deg
   if abs(res(l)~=0)
     a(k)=a(k)+res(l)*exp(pol(l)*k);
   end;
  end; % l loop
end; % k loop

end;   %function
```

DISTRIBUTION LIST

An Approach to Characterising Ground Probing Target Echoes for Landmine Recognition

Dragana Carevic

AUSTRALIA

DEFENCE ORGANISATION

Task Sponsor
DGFD(L)

S&T Program
Chief Defence Scientist
FAS Science Policy
AS Science Corporate Management
} shared copy
Director General Science Policy Development
Counsellor Defence Science, London (Doc Data Sheet)
Counsellor Defence Science, Washington (Doc Data Sheet)
Scientific Adviser to MRDC Thailand (Doc Data Sheet)
Director General Scientific Advisers and Trials/Scientific Adviser Policy and Command (shared copy)
Navy Scientific Adviser (Doc Data Sheet and distribution list only)
Scientific Adviser - Army
Air Force Scientific Adviser (Doc Data Sheet and distribution list only)
Director Trials

Aeronautical and Maritime Research Laboratory
Director

Electronics and Surveillance Research Laboratory
Director

Chief of .Surveillance Systems Division
Head Sensor Applications
Task Manager: Dr Ian Chant
Author(s): Dr Dragana Carevic

DSTO Library
Library Fishermens Bend
Library Salisbury (2 copies)
Australian Archives
Library, MOD, Pyrmont (Doc Data sheet only)

Library, MOD, HMAS Stirling only

Capability Development Division

Director General Maritime Development (Doc Data Sheet only)
Director General Land Development
Director General C3I Development (Doc Data Sheet only)

Army

ABCA Office, G-1-34, Russell Offices, Canberra (4 copies)
SO (Science), DJFHQ(L), MILPO Enoggera, Queensland 4051 (Doc Data Sheet only)
NAPOC QWG Engineer NBCD c/- DENGRS-A, HQ Engineer Centre Liverpool Military Area, NSW 2174 (Doc Data Sheet only)

Intelligence Program

DGSTA Defence Intelligence Organisation

Corporate Support Program (libraries)

OIC TRS, Defence Regional Library, Canberra
Officer in Charge, Document Exchange Centre (DEC), (Doc Data Sheet only)
*US Defence Technical Information Center, 2 copies
*UK Defence Research Information Centre, 2 copies
*Canada Defence Scientific Information Service, 1 copy
*NZ Defence Information Centre, 1 copy
National Library of Australia, 1 copy

UNIVERSITIES AND COLLEGES

Australian Defence Force Academy
Library
Deakin University, Serials Section (M list), Deakin University Library
Senior Librarian, Hargrave Library, Monash University
Librarian, Flinders University

OTHER ORGANISATIONS

NASA (Canberra)
AGPS
State Library of South Australia
Parliamentary Library, South Australia

OUTSIDE AUSTRALIA

ABSTRACTING AND INFORMATION ORGANISATIONS

INSPEC: Acquisitions Section Institution of Electrical Engineers
Library, Chemical Abstracts Reference Service
Engineering Societies Library, US
Materials Information, Cambridge Scientific Abstracts, US
Documents Librarian, The Center for Research Libraries, US

INFORMATION EXCHANGE AGREEMENT PARTNERS

Acquisitions Unit, Science Reference and Information Service, UK
Library - Exchange Desk, National Institute of Standards and Technology, US

SPARES (5 copies)

Total number of copies:

DEFENCE SCIENCE AND TECHNOLOGY ORGANISATION
DOCUMENT CONTROL DATA

1. PRIVACY MARKING/CAVEAT (OF DOCUMENT)

2. TITLE

An Approach to Characterising Ground Probing Target Echoes for Landmine Recognition

3. SECURITY CLASSIFICATION (FOR UNCLASSIFIED REPORTS THAT ARE LIMITED RELEASE USE (L) NEXT TO DOCUMENT CLASSIFICATION)

Document (U)
Title (U)
Abstract (U)

4. AUTHOR(S)

Dragana Carevic

5. CORPORATE AUTHOR

Electronics and Surveillance Research Laboratory
PO Box 1500
Salisbury SA 5108 Australia

6a. DSTO NUMBER	6b. AR NUMBER	6c. TYPE OF REPORT	7. DOCUMENT DATE
DSTO-TR-0680	AR-010-561	Technical Report	June 1998

8. FILE NUMBER	9. TASK NUMBER	10. TASK SPONSOR	11. NO. OF PAGES	12. NO. OF REFERENCES
Z-1208(3)152	ADL 95/072	DGFD(L)	36	30

13. DOWNGRADING/DELIMITING INSTRUCTIONS

14. RELEASE AUTHORITY

Chief, Tactical Surveillance Systems Division

15. SECONDARY RELEASE STATEMENT OF THIS DOCUMENT

Approved for public release

OVERSEAS ENQUIRIES OUTSIDE STATED LIMITATIONS SHOULD BE REFERRED THROUGH DOCUMENT EXCHANGE CENTRE, DIS NETWORK OFFICE, DEPT OF DEFENCE, CAMPBELL PARK OFFICES, CANBERRA ACT 2600

16. DELIBERATE ANNOUNCEMENT

No Limitations

17. CASUAL ANNOUNCEMENT Yes

18. DEFTEST DESCRIPTORS

Ground penetrating radar
Mine detection
Land mines
Radar signatures
Radar targets

19. ABSTRACT

This report investigates an approach to characterising Ground Probing Radar (GPR) backscatter echoes from landmines using linear combinations of exponentially damped sinusoids. The GPR signatures of surrogate landmines and PVC cylinders buried in dry sand are measured using impulse radar system with centre frequency of 1.4 GHz and a 90% bandwidth. The GPR signal parameters are represented as sets of complex poles computed from a series of neighbouring signatures recorded over each target type. The algorithm proposed by Kumaresan and Tufts which uses backward linear prediction and the low-rank data matrix approximation based on singular value decomposition is applied for this computation.

The performance of the Kumaresan and Tufts (KT) algorithm is compared with that of the Prony method when both techniques are applied to modelling simulated signals. It is concluded that the KT method provides more stable pole estimates.

Two approaches to determining the order of the model are examined and compared for simulated and real data.

The results show that the poles corresponding to different target types form clusters in the two-dimensional α-f space (where α is the pole damping factor and f is the pole frequency). This indicates that these pole clusters can be used for the recognition of landmines.